Lifetime Control in Irradiated and Annealed Cz n-Si: Role of Divacancy-Oxygen Defects

Mykola Kras'ko, Andrii Kolosiuk,* Vasyl Voitovych, and Vasyl Povarchuk

The behavior of the nonequilibrium charge carrier lifetime (τ) in Czochralski-grown (Cz) n-Si after a low-dose ^{60}Co gamma or 1 MeV electron irradiation and subsequent annealing are investigated. Irradiated samples with different doping levels (free-electron concentration $n_0 \approx 10^{14}$–10^{16} cm^{-3}) are isochronally annealed at temperatures between 20 and 380 °C. It is found that τ significantly decreases after annealing in the range $\approx$180–280 °C, and this effect is stronger in low-resistivity n-Si. It is shown that change in τ in the annealing range of 180–380 °C is caused by the divacancy-oxygen (V_2O) complexes. The Shockley–Read–Hall (SRH) theory is used to describe the experimental data. It is determined that the V_2O formation is characterized by the activation energy of 1.24 ± 0.04 eV and the frequency factor of $(1 \pm 0.5) \times 10^9$ s^{-1}, and their annealing is characterized by the activation energy of 1.54 ± 0.09 eV and the frequency factor of $(2.9 \pm 0.6) \times 10^{10}$ s^{-1}. The values of hole capture cross-section (σ_p) by the single- and double-charged acceptor states of V_2O are obtained as $(5 \pm 2) \times 10^{-13}$ and $(8 \pm 4) \times 10^{-12}$ cm^2, respectively.

1. Introduction

The V_2O is one of the dominant electrically active vacancy- and oxygen-related defects in irradiated silicon. It has been suggested that V_2O complex acts as deep-level acceptor and is responsible for degradation of silicon particle detectors.[1–3] The V_2O was first identified as an irradiation-induced defect in Cz silicon after high-dose electron irradiation.[4] Later, it was shown that V_2O can be formed in low-dose irradiated Cz and diffusion-oxygenated float-zone (DOFZ) silicon after annealing above 200 °C when a mobile divacancy (V_2) is trapped by interstitial oxygen (O_i) atom ($V_2 + O_i \rightarrow V_2O$).[5–12] This defect remains stable up to $\approx$300 °C. The electronic properties of V_2O are very similar to V_2. A two new levels with positions at $\approx E_c - 0.23$ and $\approx E_c - 0.47$ eV in n-type material have been assigned to double- and single-negative acceptor states of the V_2O.[5–8] In p-type material, a new level at $\approx E_v + 0.23$ eV was identified as the donor state $(+/0)$ of V_2O.[9–12] Simultaneously, level at $\approx E_v + 0.08$ eV

Dr. M. Kras'ko, Dr. A. Kolosiuk, Dr. V. Voitovych, Dr. V. Povarchuk
Laboratory of Radiation Technologies
Institute of Physics of the NAS of Ukraine
46 Nauki Ave., Kyiv 03028, Ukraine
E-mail: krasko@iop.kiev.ua; anjey.k@gmail.com

was assigned to double donor state $(2+/+)$ of V_2O.[10,12]

Existing investigations were mostly directed to studying the properties of V_2O. However, the influence of V_2O defects on the change of integral parameters (in particular, the carrier lifetime) of Cz Si has not been sufficiently studied. At the same time, it was shown that there is a connection between the changes in τ and the V_2O formation in γ-irradiated Cz n-Si after annealing in the range $\approx$200–400 °C and also during electron irradiation in the same temperature range.[13,14] Having high thermal stability and deep electronic levels in the band gap of silicon, V_2O defects can be effective recombination centers that determine the behavior of silicon devices operational characteristics.

In the present study, the degradation of carrier lifetime in ^{60}Co γ- or 1 MeV electron-irradiated Cz n-Si after isochronal annealing in the temperature range of 20–380 °C is investigated. In this context, we study in detail the range 180–380 °C to determine the role of V_2O defects in the change of recombination properties of irradiated and annealed Cz n-Si.

2. Experimental Section

2.1. Samples, Irradiation, and Annealing

The samples (typical size of $\approx$10 mm $\times$ 5 mm $\times$ 2.5 mm) Cz silicon of n-type (doped with phosphorus) with different $n_0 \approx 10^{14}$–10^{16} cm^{-3} were used. The n_0 was determined from the Hall effect measurements. The doping level determined the electron filling of the defect level (by changing the Fermi level) and, accordingly, its recombination activity. In oxygen-rich n-Si, the levels of single- and double-charged acceptor states of V_2O were identified.[5–8] Using samples with different n_0, we studied the contribution of each of them in τ change.

The concentrations of interstitial oxygen $[O_i]$ and substitutional carbon $[C_s]$ atoms in the samples were $\approx(6$–$8) \times 10^{17}$ and $\leq 4 \times 10^{16}$ cm^{-3}, respectively. The $[O_i]$ and $[C_s]$ in the samples were determined from measurements of the intensity of the absorption bands at 1107 and 607 cm^{-1} with the use of the calibration coefficients of 3.14×10^{17} and 0.94×10^{17} cm^{-2}, respectively.

The samples were irradiated at room temperature with γ-rays from a ^{60}Co source ($E_\gamma \approx 1.25$ MeV) to a dose (Φ) of 7×10^{14} cm^{-2} (intensity of irradiation $J_\gamma \approx 2 \times 10^{11}$ photons

$cm^{-2} s^{-1}$) or 1 MeV electrons to a dose of $1 \times 10^{13} cm^{-2}$ ($J_e \approx 3 \times 10^{11}$ electrons $cm^{-2} s^{-1}$).

Isochronal (20 min) anneals of the irradiated samples were carried out in an open furnace at temperatures between 20 and 380 °C (20 °C step), where the formation and annealing of V_2O complexes occur.

2.2. Carrier Lifetime Measurement and Analysis of Results

The carrier lifetime in the samples was derived at room temperature from the relaxation of the nonequilibrium photoconductivity. A schematic diagram of the experimental setup is shown in **Figure 1**. A GaAs light-emitting diode (LED) (wavelength of 940 nm) pulse was used for the excess carriers generation (Δn is the concentration of nonequilibrium carriers). When passing through a sample of direct current, the voltage drop on it was proportional to the carrier concentration. This makes it possible to observe the relaxation processes directly on the oscilloscope. By changing the amplitude of electrical pulses that are fed to the LED, we can change Δn. A low excitation level, typically $\Delta n/n_0 \approx 1\%$, was employed. The relative error of τ value determination did not exceed ±10% (error bars on experimental dependences).

For all the investigated samples, the initial carrier lifetime (τ_0) was ≈100 µs. For lifetime measurements, gallium–indium (InGa) eutectic was applied as an ohmic contact. The contacts were removed before each annealing step by mechanically polishing and subsequent etching for 1 min in CP4 (HF:HNO$_3$:C$_2$H$_4$O$_2$ [3:5:3]). After annealing, the samples were etched in HF to remove possible oxide layers, and new contacts were formed on the same surfaces as before. A part of the non-irradiated samples was used as control material. They were subjected to the same procedures for annealing and measurements as irradiated samples to control the possible effects of hydrogen (can be introduced at etching in CP4) or the other contaminants. **Figure 2** shows dependences of τ on the temperature of 20 min isochronal annealing (T_{ann}) in the range of 20–320 °C for nonirradiated Cz n-Si with different n_0. It was seen that τ in annealed control samples almost does not change in comparison with τ_0 ($T_{ann} = 20$ °C in Figure 2).

For the analysis of experimental data, the Shockley–Read–Hall (SRH) theory was used.[15] In our case (n-Si, small concentration of traps, $\Delta n << n_0$, the carrier recombination occurs through a level located in the upper half of the bandgap), the lifetime of nonequilibrium charge carriers was determined by the lifetime of holes (minority charge carriers in n-Si), and the following expression of the SRH recombination is valid for the calculation of τ

$$\tau_i = (\sigma_{p,i} v_p [N_i])^{-1} \left[1 + \frac{N_c \exp(-E_i/k_B T)}{n_0} \right] \quad (1)$$

where $\sigma_{p,i}$ is the cross section of hole capture by the ith recombination center; v_p is the thermal velocity of holes; $[N_i]$ is the concentration of the ith center with the electronic level E_i; N_c is the effective density of states in the conduction band; k_B is Boltzmann's constant; and T—the absolute temperature.

At the same time, the total change of carrier lifetime is expressed by a sum of reciprocal τ_i as

$$\tau^{-1} - \tau_0^{-1} = \sum_i \tau_i^{-1} \quad (2)$$

where τ_0 is the initial carrier lifetime; τ is the carrier lifetime in irradiated and annealed silicon.

3. Results and Discussion

The change of τ in irradiated and then annealed silicon means a change in the concentration of the dominant recombination of radiation-induced defects or the formation of new recombination defects. Therefore, our study included two successive stages. We first investigated the τ degradation in irradiated Cz n-Si, and further, we studied the influence of isochronal annealing on the behavior of τ in irradiated samples.

3.1. Irradiation-Induced Change of Carrier Lifetime

Figure 3 shows the typical dose dependences of $\Delta\tau_{irr}^{-1} = \tau^{-1} - \tau_0^{-1}$ for ^{60}Co γ-irradiated Cz n-Si with a different n_0.
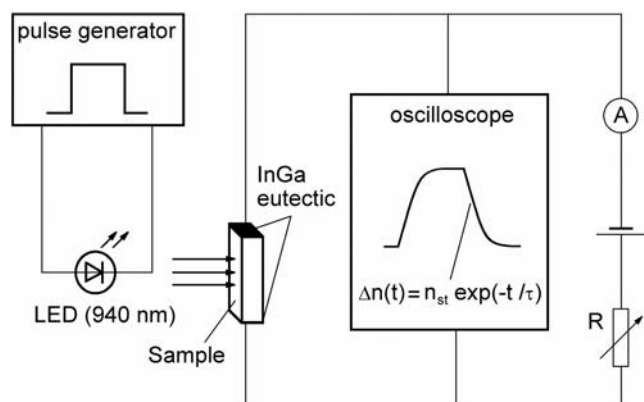

Figure 1. A schematic diagram of the experimental setup to determine the nonequilibrium charge carrier lifetime.
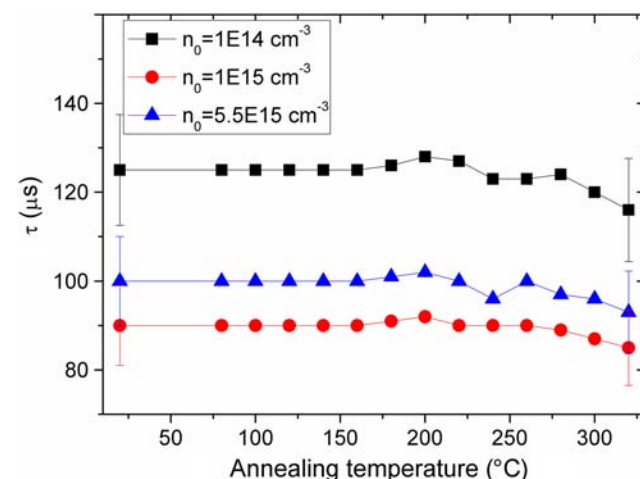

Figure 2. τ as a function the temperature of 20 min isochronal annealing (T_{ann}) for nonirradiated Cz n-Si with different doping levels.
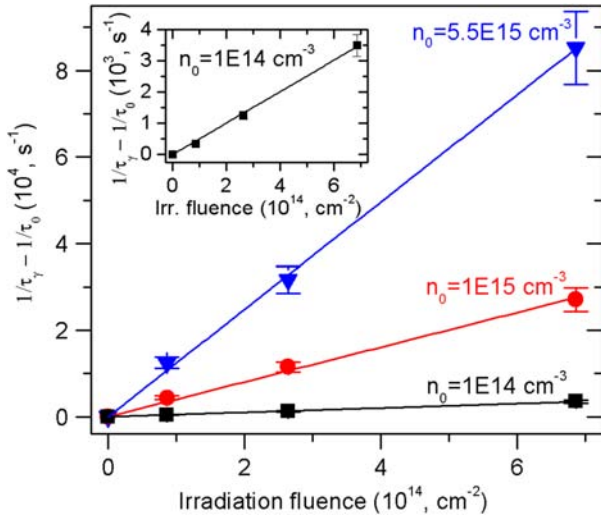
Figure 3. Dose dependences of $\Delta\tau_{irr}^{-1} = \tau^{-1} - \tau_0^{-1}$ for ^{60}Co γ-irradiated Cz n-Si with different doping levels. The inset shows the same dependence for a sample with $n_0 = 1 \times 10^{14}$ cm^{-3} on a larger scale. The symbols show the experimental data and the curves show their linear approximations.

We see that $\Delta\tau_{irr}^{-1}$ increases linearly to a dose of $\approx 7 \times 10^{14}$ cm^{-2} for all samples. This corresponds to the condition of small concentration of traps, when concentration of radiation-induced defects responsible for τ degradation is low in comparison with n_0 and the concentration of impurity atoms involved in the formation of these defects.

Figure 4 shows the dependence of $\Delta\tau_{irr}^{-1}(n_0)$ for γ-irradiated samples, which is increasing in the investigated range of n_0 (τ degradation occurs most strongly in low-resistivity n-Si). It is known that the vacancy-oxygen (VO) center (acceptor level of $E_c - 0.17$ eV) is mostly responsible for the τ degradation in ^{60}Co γ-irradiated Cz n-Si with doping levels of $10^{13} - 10^{17}$ cm^{-3}.[16–19]
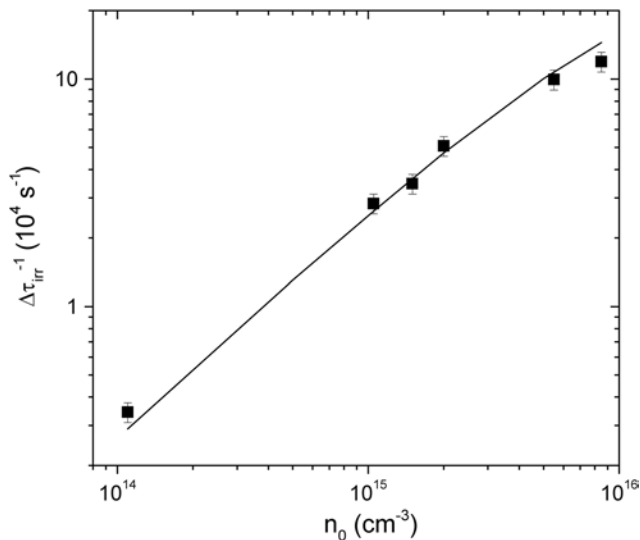

Figure 4. $\Delta\tau_{irr}^{-1}$ as a function of n_0 for ^{60}Co γ-irradiated with $\Phi \approx 7 \times 10^{14}$ cm^{-2} Cz n-Si. The symbols show the experimental data and the solid curve shows calculated SRH lifetime for VO contribution.

This is also confirmed by our calculations. From Equation (2), taking into account Equation (1), we obtain

$$\Delta\tau_{irr}^{-1} = \tau_{VO}^{-1} = \sigma_{p,VO}\upsilon_p[VO]_{irr}\left(1 + \frac{N_c\exp(-E_{VO}/k_BT)}{n_0}\right)^{-1} \quad (3)$$

where $E_{VO} = E_c - 0.17$ eV.

In Equation (3), the unknown parameters are $\sigma_{p,VO}$ and $[VO]_{irr}$. For the case of ^{60}Co γ-irradiation, the introduction rate (η) of VO in Cz n-Si with doping levels $10^{14} - 10^{16}$ cm^{-3} is almost constant and the η_{VO} value is $\approx 4 \times 10^{-4}$ cm^{-1}.[16,17] It follows that, after irradiation at the fluence—7×10^{14} cm^{-2}, $[VO]_{irr} \approx 2.8 \times 10^{11}$ cm^{-3}. The solid line on dependence $\Delta\tau_{irr}^{-1}(n_0)$ (Figure 4) is the result of the calculation by Equation (3) in which only $\sigma_{p,VO}$ is the fitting parameter. The calculation and the experiment are in good agreement if $\sigma_{p,VO} = (2.0 \pm 0.4) \times 10^{-13}$ cm^2 that is similar to the results obtained in previous research.[16,17,20] In the investigated range of $n_0 - \eta_{VO} \approx$ const, therefore, as can be seen from Equation (3), the growth of $\Delta\tau_{irr}^{-1}(n_0)$ is due to an increase of electron filling of the VO acceptor level with increasing of n_0.

We also note that the influence of other radiation-induced defects (in particular V_2 and VP) on τ degradation in ^{60}Co γ-irradiated Cz n-Si is negligible.[16–19] However, in the case of V_2, this effect becomes noticeable in Cz n-Si after high-energy (≥ 6 MeV) electron irradiation as a result of a decrease in the ratio η_{VO}/η_{V_2}.[14,20–22] For example, the ratio $\eta_{VO}/\eta_{V_2} \approx 80$ for ^{60}Co γ-irradiation and $\eta_{VO}/\eta_{V_2} \approx 4$–5 for 3.5 MeV electron irradiation.[16,21,22]

3.2. Postirradiation Isochronal Annealing of Carrier Lifetime

3.2.1. Experimental Results

Figure 5 shows typical dependences of $\Delta\tau^{-1} = \tau^{-1} - \tau_0^{-1}$ on the temperature of 20 min isochronal annealing in the range of 20–380 °C for ^{60}Co γ-irradiated Cz n-Si with a different n_0.

As shown in Figure 5, two characteristic features are observed on dependences $\Delta\tau^{-1}(T_{ann})$ for all samples. An increase in annealing temperature up to ≈ 180 °C does not lead to a noticeable change of τ. However, the thermal treatment in the temperature range of 180–380 °C leads to significant (peak-like) changes: first, $\Delta\tau^{-1}$ increases (accordingly, τ decreases) at 240–280 °C and then decreases to the value corresponding to ≈ 80–90% of τ_0 at ≈ 360–380 °C. There is also a tendency that the peak position is shifted to higher temperatures with an increase in n_0. In our case, this shift is about 40 °C.

The change of recombination properties of ^{60}Co γ-irradiated Cz n-Si after annealing in the temperature range of 180–380 °C (Figure 5) means an increase in the VO concentration (dominant recombination center in ^{60}Co γ-irradiated Cz n-Si, see Section 3.1) or the formation of new recombination defects that are more active than VO. The temperature range ≈ 180–300 °C is an annealing interval of V_2 in Cz and DOFZ silicon.[5–12] At ^{60}Co γ-irradiation, the introduction rate of VO in Cz n-Si at room temperature is approximately two orders of magnitude higher than that for η_{V_2}.[16,21] Therefore, the additional VO formation due to the possible V_2 dissociation ($V_2 + 2O_i \rightarrow 2V + 2O_i \rightarrow 2VO$) cannot have a noticeable impact on the τ degradation.[16,21]

ADVANCED
SCIENCE NEWS
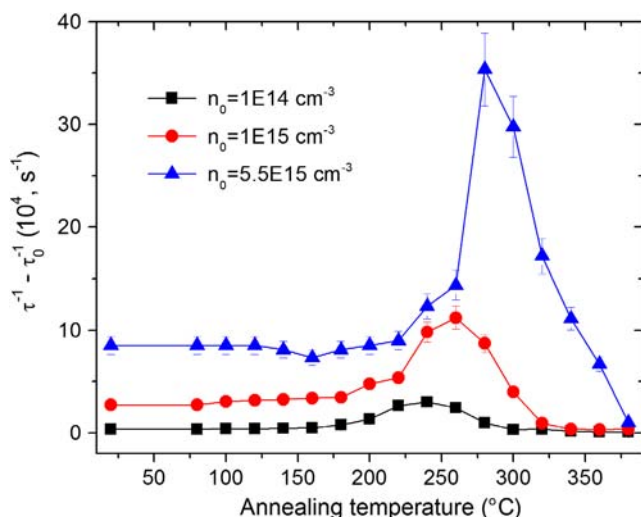www.advancedsciencenews.com

physica
pss status solidi a
www.pss-a.com

Figure 5. $\Delta\tau^{-1} = \tau^{-1} - \tau_0^{-1}$ as a function the temperature of 20 min isochronal annealing (T_{ann}) for ^{60}Co γ-irradiated Cz n-Si with different doping levels. τ_0 is the initial carrier lifetime and τ is the carrier lifetime in samples subjected to γ-irradiation ($\Phi \approx 7 \times 10^{14}$ cm^{-2}) and subsequent annealing steps.

Thus, the V$_2$ annealing can lead to the formation of the V$_2$-related defect, and this is demonstrated by the following experiment.

Cz n-Si sample $\approx$2.5 mm thick was irradiated by 1 MeV electrons at room temperature from the side of one of its largest facets, whereas the τ measurements were made on both. The comparison of the deep level transient spectroscopy (DLTS) spectra (see Figure 1 in the study by David et al.[23]) for the 1 MeV electron irradiated and shadow sides of Cz n-Si sample $\approx$2.5 mm thick make it evident that peaks assigned to double-negative (E2, $E_c - 0.23$ eV) and single-negative (E3, $E_c - 0.42$ eV) acceptor states of the V$_2$ can be observed only on the irradiated side of the sample. At the same time, the peak related to VO center is present in both spectra. However, the [VO] on the shadow side is approximately an order of magnitude lower than that of the irradiated one. In this case, if the τ change in the range 180–380 °C (Figure 5) is caused by the V$_2$-related defect, it will be absent on the shadow side of the sample.

Figure 6 compares the experimental dependences $\Delta\tau^{-1}(T_{ann})$ in the range of 20–350 °C for the 1 MeV electron-irradiated (front) and shadow (back) sides of the sample.

As one can see from Figure 6, the ratio $\Delta\tau^{-1}_{irr}$ ($\Delta\tau^{-1}_{irr}$ – the value of $\Delta\tau^{-1}$ after irradiation, $T_{ann} = 20$ °C in Figure 6) for these sides is the same ($\approx$10) as the ratio [VO] on Figure 1 in the study by David et al.[23], and the relative peak height $(\Delta\tau^{-1}_{peak} - \Delta\tau^{-1}_{irr})/\Delta\tau^{-1}_{irr}$ ($\Delta\tau^{-1}_{peak}$ – the value of $\Delta\tau^{-1}$ corresponds to the peak on these dependences, $T_{ann} = 240$ °C in Figure 6) for the irradiated side is much larger than that for the shadow one ($\approx$2 and 0.5, respectively). The V$_2$ are detected in the near-surface layer of the irradiated side in contrast to the shadow one. This could mean that the formation of V$_2$-related defects leads to the τ degradation after annealing in the temperature range of 180–300 °C both for the electron-irradiated side of the sample (Figure 6) and for γ-irradiated samples (Figure 5). It should be noted that in the experiment we measure a bulk
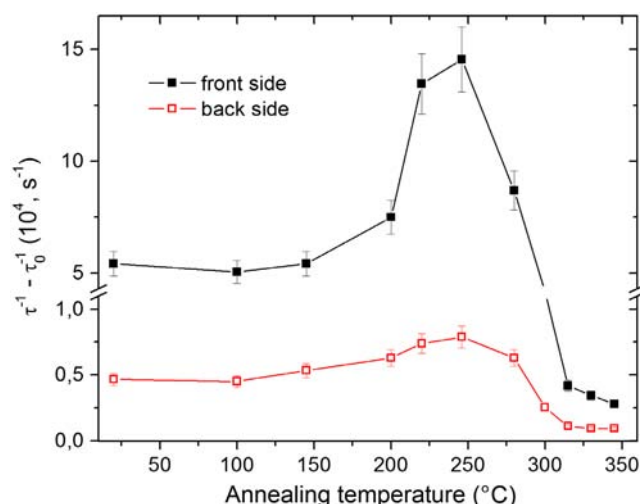

Figure 6. $\Delta\tau^{-1}$ as a function of T_{ann} for 1 MeV electron irradiated with $\Phi = 1 \times 10^{13}$ cm^{-2} (front side) and shadow (back side) sides of Cz n-Si ($n_0 \approx 1 \times 10^{15}$ cm^{-3}) sample $\approx$2.5 mm thick.

carrier lifetime (the recombination region thickness is about 0.15–0.50 mm); thus, this fact explains the presence of a small peak on dependence $\Delta\tau^{-1}(T_{ann})$ for the shadow side in Figure 6.

It is most likely that these V$_2$-related defects are the V$_2$O complexes. First, DLTS and Laplace DLTS studies of the kinetics of V$_2$ annealing and V$_2$O formation in DOFZ and Cz n-Si show that the transformation of V$_2$ to V$_2$O occurs with an almost one-to-one proportionality.[5–8] Second, the peak-like change of $\Delta\tau^{-1}$ (Figure 5 and 6) and the change in the V$_2$O concentration in Cz n-Si are clearly correlated in the annealing range of 180–380 °C.[7] In an earlier work, from the analysis of the temperature dependence of τ in γ-irradiated and annealed Cz n-Si ($n_0 = 7 \times 10^{13}$ cm^{-3}), it was found that the acceptor with level E_c—0.45 eV is responsible for τ degradation in the range $\approx$200–300 °C.[18] It is noted that the level of this defect is practically the same as the level of V$_2$O(−/0).

3.2.2. SRH Description of Carrier Lifetime Change in Irradiated and Annealed Cz n-Si

From the viewpoint of our previous considerations, the total change of τ in irradiated and annealed Cz n-Si is expressed by the sum of contributions of VO (see Section 3.1) and V$_2$O (see Section 3.2.1). According to Equation (2), we obtain

$$\Delta\tau^{-1} = \tau_{VO}^{-1} + \tau_{V_2O}^{-1} \tag{4}$$

The $\Delta\tau_{VO}^{-1}$ is calculated by Equation (3). The V$_2$O defect is a multi-charge center. In our samples ($n_0 \geq 1 \times 10^{14}$ cm^{-3}), the Fermi-level position at room temperature is higher than the V$_2$O(−/0) level. This means that the influence of V$_2$O on τ will be determined only by double- and single-negative acceptor levels of V$_2$O:

$$\Delta\tau_{V_2O}^{-1} = \tau_{V_2O(2-/-)}^{-1} + \tau_{V_2O(-/0)}^{-1} \tag{5}$$

According to Equation (1)

$$\tau_{V_2O(2-/-)}^{-1} = \sigma_{p,V_2O(2-/-)}\upsilon_p[V_2O]f_{2-}$$
$$\times \left(1 + \frac{N_c \exp(-E_{V_2O(2-/-)}/k_B T)}{n_0}\right)^{-1} \quad (6)$$

and

$$\tau_{V_2O(-/0)}^{-1} = \sigma_{p,V_2O(-/0)}\upsilon_p[V_2O](1-f_{2-})$$
$$\times \left(1 + \frac{N_c \exp(-E_{V_2O(-/0)}/k_B T)}{n_0}\right)^{-1} \quad (7)$$

where $E_{V_2O(2-/-)} = E_c - 0.23$ eV, $E_{V_2O(-/0)} = E_c - 0.47$ eV, f_{2-} is the Fermi distribution function which describes filling of the $V_2O(2-/-)$ level.

In the general case $\tau_i^{-1} \approx [N_i]$ (see Equation (1)); therefore, the annealing behavior of τ in Figure 5 will be determined by the change in the V_2O and VO concentrations. Moreover, the annealing behavior of τ in the temperature range of 180–380 °C on the experimental dependences $\Delta\tau^{-1}(T_{ann})$ in Figure 5 was caused by the formation (from 180 to 240–280 °C) and annealing (from 240–280 to 380 °C) of V_2O defects. Also, the VO annealing occurs at $T_{ann} > 300$ °C.[21]

The corresponding system of kinetic equations, which describes the processes of V_2O formation $(V_2 + O \rightarrow V_2O)$ and subsequent annealing, is as follows

$$\begin{cases} \frac{d[V_2]}{dt} = -c_{V_2O}[V_2] \\ \frac{d[V_2O]}{dt} = c_{V_2O}[V_2] - c_{V_2O}^{ann}[V_2O] \end{cases} \quad (8)$$

with a temperature-dependent rate constant for formation $c_{V_2O} = c_0 \exp(-E_a/k_B T)$ and annealing $c_{V_2O}^{ann} = c_0^{ann} \exp(-E_a^{ann}/k_B T)$ of V_2O.

The solution of system Equations (8) with the initial condition $[V_2](t=0) = [V_2]_{irr}$ and $[V_2O](t=0) = 0$ is as follows

$$[V_2O] = \frac{[V_2]_{irr}}{(c_{V_2O}^{ann}/c_{V_2O} - 1)} \times \left(\exp(-c_{V_2O}t) - \exp(-c_{V_2O}^{ann}t)\right) \quad (9)$$

where t – the time of isochronal annealing.

The kinetic equation for VO annealing

$$\frac{d[VO]}{dt} = -c_{VO}^{ann}[VO] \quad (10)$$

The solution of Equation (10) with the initial condition $[VO](t=0) = [VO]_{irr}$ is as follows

$$[VO] = [VO]_{irr} \times \exp(-c_{VO}^{ann}t) \quad (11)$$

Figure 7 demonstrates the dependence of peak height on dependences $\Delta\tau^{-1}(T_{ann})$ in Figure 5 $(\Delta\tau_{peak}^{-1} - \Delta\tau_{irr}^{-1})(n_0)$ as a function of n_0 for all investigated samples. Curve 1 corresponds to the maximum contribution of V_2O in the total τ change when all V_2 are transformed to V_2O. Although the dependence $(\Delta\tau_{peak}^{-1} - \Delta\tau_{irr}^{-1})(n_0)$ is growing (curve 1 in Figure 7 demonstrates that an increase in n_0 from 1×10^{14} to 8×10^{15} cm^{-3} induces an approximately eightfold increase of $(\Delta\tau_{peak}^{-1} - \Delta\tau_{irr}^{-1})$); however,
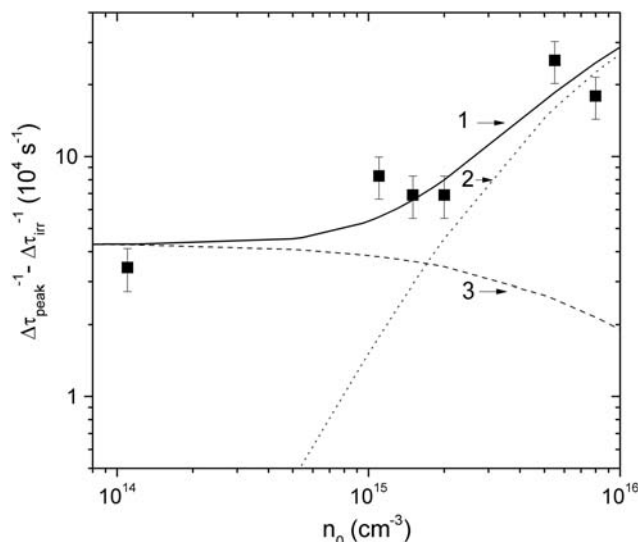

Figure 7. Peak height on dependences $\Delta\tau^{-1}(T_{ann})$ in Figure 5 $(\Delta\tau_{peak}^{-1} - \Delta\tau_{irr}^{-1})$ as a function of n_0 for all investigated samples ($\Delta\tau_{peak}^{-1}$ is the value of $\Delta\tau^{-1}$ corresponds to the peak on these dependences, $T_{ann} = 240$–280 °C in Figure 5; $\Delta\tau_{irr}^{-1}$ is the value of $\Delta\tau^{-1}$ after irradiation, $T_{ann} = 20$ °C in Figure 5). The symbols shows the experimental data and the lines show the calculated SRH lifetime for V_2O contribution: 1) cumulative, 2) $V_2O(2-/-)$, and 3) $V_2O(-/0)$.

this growth occurs most strongly in low-resistivity n-Si ($n_0 > 5 \times 10^{14}$ cm^{-3}).

Using Equations (5–7) for analysis of experimental data in Figure 7, we can estimate the values of σ_p for $V_2O(2-/-)$ and $V_2O(-/0)$ and, accordingly, the contribution of these defects in the change of τ. At ^{60}Co γ-irradiation, the ratio of $\eta_{VO}/\eta_{V_2} \approx 80$.[16,21] Then, after irradiation at the fluence— 7×10^{14} cm^{-2}, we obtain that the V_2 concentration after irradiation ($[V_2]_{irr}$) is $\approx 3.5 \times 10^9$ cm^{-3}. The solid line on dependence $(\Delta\tau_{peak}^{-1} - \Delta\tau_{irr}^{-1})(n_0)$ (curve 1 in Figure 7) shows the cumulative contribution of $V_2O(2-/-)$ (curve 2 in Figure 7) and $V_2O(-/0)$ (curve 3 in Figure 7) calculated by Equations (5–7). The calculation and the experiment are in satisfactory agreement if $\sigma_{p,V_2O(-/0)} = (5 \pm 2) \times 10^{-13} \times 10^{-13}$ cm^2 and $\sigma_{p,V_2O(2-/-)} = (8 \pm 4) \times 10^{-12}$ cm^2. In addition, the calculation shows that τ is controlled by the single-negative V_2O level in high-resistivity n-Si ($n_0 < 5 \times 10^{14}$ cm^{-3}, curve 3 in Figure 7) and double-negative V_2O level in low-resistivity n-Si ($n_0 > 5 \times 10^{15}$ cm^{-3}, curve 2 in Figure 7). The growth of $(\Delta\tau_{peak}^{-1} - \Delta\tau_{irr}^{-1})(n_0)$ (curve 1 in Figure 7) is due to an increase in electron filling of the $V_2O(2-/-)$ level for which σ_p is large than that for $V_2O(-/0)$.

Using the known parameters for VO and V_2O (**Table 1**) and experimental data (Figure 5), we calculated the activation energies and frequency factors for formation and annealing of

Table 1. Defect states considered in the SRH calculation.

Defect	Level [eV]	σ_p at 293 K [cm^2]
VO(−/0)	$E_c - 0.17$	$(2.0 \pm 0.4) \times 10^{-13}$
$V_2O(2-/-)$	$E_c - 0.23$	$(8 \pm 4) \times 10^{-12}$
$V_2O(-/0)$	$E_c - 0.47$	$(5 \pm 2) \times 10^{-13}$

Table 2. Activation energies and frequency factors for formation and annealing of V_2O and annealing of VO determined from experimental data.

n_0, [cm^{-3}]	1×10^{14}	1×10^{15}	5.5×10^{15}
V_2O formation			
E_a [eV]	1.2	1.24	1.27
c_0 [s^{-1}]	1.5×10^9	1.5×10^9	5.0×10^8
V_2O annealing			
E_a^{ann} [eV]	1.45	1.52	1.63
c_0^{ann} [s^{-1}]	2.2×10^{10}	3.3×10^{10}	3.5×10^{10}
VO annealing			
E_a^{ann} [eV]	1.6	1.55	1.62
c_0^{ann} [s^{-1}]	5.6×10^9	5.6×10^9	5.6×10^9

V_2O [Equation (5–7) and (9)] and annealing of VO [Equation (3) and (11)]. The obtained data are given in **Table 2** and correspond to the best agreement of theory with the experiment.

Figure 8 demonstrates the result of the description (lines) of the experimental dependences $\Delta\tau^{-1}(T_{ann})$ with the parameters for VO and V_2O defects that are shown in Table 1 and 2. It is noted that the V_2O and VO defects are annealed at ≈ 300–$380\,°C$. Therefore, we have separated the influence of VO and V_2O on τ change to correctly determine the V_2O contribution. For this purpose, the VO annealing rate constant $c_{VO} = 5.6 \times 10^9 \exp(-1.7/k_BT)$ is taken from Ref. [21] as a basis

and, for our experimental data, only the E_a value is slightly corrected (see Table 2). As shown in Table 2, the average E_a for the V_2O formation is 1.25 ± 0.05 eV. Our results concerning the V_2O formation agree well with experimental data where it was found that both the V_2 annealing and the V_2O formation are characterized by the same activation energy of about 1.3 eV.[8,24] The E_a^{ann} of 1.54 ± 0.09 eV for the V_2O annealing (see Table 2) is similar to the theory, but less than ≈ 2 eV in the experiment.[25,26]

Using data in Figure 5 of Ref. [7] for changes upon isochronal annealing in concentrations of V_2 and V_2O in electron-irradiated Cz n-Si, we got the $c_{V_2O}(T)$ for the V_2O formation and annealing which are very close to our results. It is also noted that both the tendency to increase E_a and E_a^{ann} for V_2O (Table 2) and the shift of the peak position on dependences $\Delta\tau^{-1}(T_{ann})$ to higher temperatures with increasing n_0 (Figure 5) are correlated. Probably, the charge state of the V_2O plays a key role in this situation. This question is not being studied in our work.

Finally, comparing the absolute values of the maximum influence of V_2O (curve 1 in Figure 7) and VO (Figure 4) on τ degradation in irradiated and annealed Cz n-Si in the investigated range of n_0, we see that the V_2O contribution on τ degradation is larger when compared with the VO although the ratio of η_{VO} and η_{V_2} (and, therefore, the maximal concentration of V_2O) is approximately two orders of magnitude. Herewith, the influence of annealing on τ degradation in irradiated Cz n-Si is much stronger for high-resistivity samples. For example, the ratio $(\Delta\tau_{peak}^{-1} - \Delta\tau_{irr}^{-1})/\Delta\tau_{irr}^{-1}$ is ≈ 10 and 3 for samples with n_0
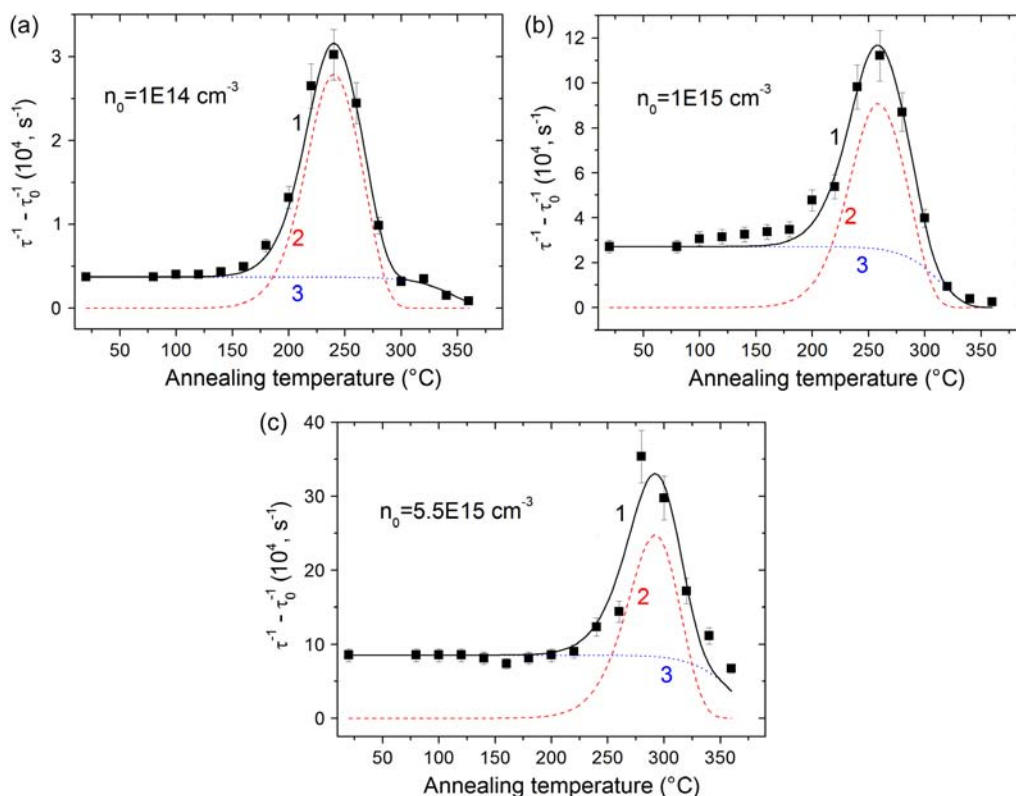

Figure 8. Comparison between experimental (symbols) and calculated (lines) dependences of $\Delta\tau^{-1}(T_{ann})$ for ^{60}Co γ-irradiated Cz n-Si with different doping levels: a) $n_0 = 10^{14}$ cm^{-3}, b) $n_0 = 10^{15}$ cm^{-3}, c) $n_0 = 5.5 \times 10^{15}$ cm^{-3}; curve 1 -cumulative contribution of V_2O (curve 2) and VO (curve 3).

of 1×10^{14} and $5.5 \times 10^{15}\,\mathrm{cm^{-3}}$, respectively. The larger value of η_{VO} is compensated by small electron filling of its level in high-resistivity n-Si ($\approx 10^{-3}$ for $n_0 = 1 \times 10^{14}\,\mathrm{cm^{-3}}$) whereas $\sigma_{p,VO} \approx \sigma_{p,V_2O(-/0)}$ and $\sigma_{p,V_2O(2-/-)} > \sigma_{p,V}$ in low-resistivity n-Si. It is also noted that the both acceptor levels of V_2 have similar band-gap positions to V_2O but smaller $\sigma_p \approx 10^{-14}\,\mathrm{cm^2}$.[20,21] Thus, the V_2O contribution to τ changes is greater than that of the V_2.

4. Conclusions

We have presented the results of a detailed study of carrier lifetime degradation in a low-dose ($\Phi = 7 \times 10^{14}\,\mathrm{cm^{-2}}$) ^{60}Co γ- and 1 MeV electron ($\Phi = 1 \times 10^{13}\,\mathrm{cm^{-2}}$) irradiated Cz n-Si ($n_0 \approx 10^{14} - 10^{16}\,\mathrm{cm^{-3}}$) after 20-min isochronal annealing in the temperature range of 20–380 °C. It is found that, at room temperature and for low excitation level ($\Delta n/n_0 = 1\%$), the τ significantly decreases after annealing in the range from 180 to 240–280 °C, and the efficiency of this process depends on doping levels in Cz n-Si (τ decreases more strongly in low-resistivity samples). We have shown that this effect is caused by V_2-related defects, which are most likely associated with the V_2O. Using the SRH theory for analysis of experimental data, it was determined that the formation and annealing of V_2O have activation energies in the range 1.24 ± 0.04 and 1.54 ± 0.09 eV, respectively. The σ_p values of $(5 \pm 2) \times 10^{-13}\,\mathrm{cm^2}$ for $V_2O(-/0)$ and $(8 \pm 4) \times 10^{-12}\,\mathrm{cm^2}$ for $V_2O(2-/-)$ are obtained. We also analyzed and compared the influence of V_2O and VO (dominant recombination center in ^{60}Co γ-irradiated Cz n-Si) on τ degradation in irradiated and annealed Cz n-Si in the investigated range of n_0. It is found that the V_2O contribution on τ degradation is larger when compared with the VO although the VO introduction rate in ^{60}Co γ- irradiated Cz n-Si at room temperature is approximately two orders of magnitude higher than that for V_2O (when all V_2 are transformed to V_2O).

Conflict of Interest

The authors declare no conflict of interest.

Keywords

[1] M. Moll, H. Feick, E. Fretwurst, G. Lindström, C. Schütze, *Nucl. Instrum. Method Phys. A* **1997**, *388*, 335.

[2] K. Gill, G. Hall, B. MacEvoy, *J. Appl. Phys.* **1997**, *82*, 126.

[3] I. Pintilie, E. Fretwurst, G. Lindström, J. Stahl, *Appl. Phys. Lett.* **2002**, *81*, 165.

[4] Y.-H. Lee, J. W. Corbett, *Phys. Rev. B* **1976**, *13*, 2653.

[5] E. V. Monakhov, B. S. Avset, A. Hallén, B. G. Svensson, *Phys. Rev. B* **2002**, *65*, 233207.

[6] G. Alfieri, E. V. Monakhov, B. S. Avset, B. G. Svensson, *Phys. Rev. B* **2003**, *68*, 233202.

[7] V. P. Markevich, A. R. Peaker, S. B. Lastovskii, L. I. Murin, J. L. Lindström, *J. Phys.: Condens. Matter* **2003**, *15*, S2779.

[8] M. Mikelsen, E. V. Monakhov, G. Alfieri, B. S. Avset, B. G. Svensson, *Phys. Rev. B* **2005**, *72*, 195207.

[9] M.-A. Trauwaert, J. Vanhellemont, H. E. Maes, A.-M. Van Bavel, G. Langouche, P. Clauws, *Appl. Phys. Lett.* **1995**, *66*, 3056.

[10] V. P. Markevich, A. R. Peaker, B. Hamilton, S. B. Lastovskii, L. I. Murin, J. Coutinho, V. J. B. Torres, L. Dobaczewski, B. G. Svensson, *Phys. Status Solidi A* **2011**, *208*, 568.

[11] N. Ganagona, B. Raeissi, L. Vines, E. V. Monakhov, B. G. Svensson, *J. Phys.: Condens. Matter* **2012**, *24*, 435801.

[12] V. P. Markevich, A. R. Peaker, B. Hamilton, S. B. Lastovskii, L. I. Murin, *J. Appl. Phys.* **2014**, *115*, 012004.

[13] M. M. Kras'ko, A. M. Kraitchinskii, V. B. Neimash, A. G. Kolosiuk, L. I. Shpinar, *Ukr. J. Phys.* **2007**, *52*, 162.

[14] V. P. Markevich, A. R. Peaker, S. B. Lastovskii, V. E. Gusakov, I. F. Medvedeva, L. I. Murin, *Solid State Phenom* **2010**, *156-158*, 299.

[15] E. Gaubas, E. Simoen, J. Vanhellemont, *ECS J. Solid State Sci. Technol.* **2016**, *5*, 3108.

[16] S. Zubrilov, S. V. Koveshnikov, *Fiz. Tekh. Poluprovodn.* **1991**, *25*, 1332.

[17] M. M. Kras'ko, V. B. Neimash, A. M. Kraitchinskii, A. G. Kolosiuk, O. M. Kabaldin, *Ukr. J. Phys.* **2008**, *53*, 683.

[18] I. I. Kolkovskii, P. F. Lugakov, V. V. Shusha, *Phys. Status Solidi A* **1984**, *83*, 299.

[19] M. Kras'ko, A. Kraitchinskii, A. Kolosiuk, V. Voitovych, R. Rudenko, V. Povarchuk, *Solid State Phenom.* **2014**, *205-206*, 323.

[20] H. Bleichner, P. Jonsson, N. Keskitalo, E. Nordlander, *J. Appl. Phys.* **1996**, *79*, 9142.

[21] S. D. Brotherton, P. Bradley, *J. Appl. Phys.* **1982**, *53*, 5720.

[22] R. Radu, I. Pintilie, L. C. Nistor, E. Fretwurst, G. Lindstroem, L. F. Makarenko, *J. Appl. Phys.* **2015**, *117*, 164503.

[23] M. L. David, E. Simoen, C. Claeys, V. Neimash, M. Kras'ko, A. Kraitchinskii, V. Voytovych, A. Kabaldin, J. F. Barbot, *Solid State Phenom.* **2005**, *108–109*, 373.

[24] P. Pellegrino, P. Lévêque, J. Lalita, A. Hallén, C. Jagadish, B. G. Svensson, *Phys. Rev. B* **2001**, *64*, 195211.

[25] J. Coutinho, R. Jones, S. Öberg, P. R. Briddon, *Physica B* **2003**, *340–342*, 523.

[26] M. Mikelsen, J. H. Bleka, J. S. Christensen, E. V. Monakhov, B. G. Svensson, *Phys. Rev. B* **2007**, *75*, 155202.